Monthly Notices of the ROYAL ASTRONOMICAL SOCIETY
MNRAS **445,** 1878–1884 (2014) doi:10.1093/mnras/stu1876

Variable emission from a gaseous disc around a metal-polluted white dwarf

D. J. Wilson,[1]★ B. T. Gänsicke,[1] D. Koester,[2] R. Raddi,[1] E. Breedt,[1] J. Southworth[3] and S. G. Parsons[4]

[1]*Department of Physics, University of Warwick, Coventry CV4 7AL, UK*
[2]*Institut für Theoretische Physik und Astrophysik, University of Kiel, D-24098 Kiel, Germany*
[3]*Astrophysics Group, Keele University, Staffordshire ST5 5BG, UK*
[4]*Departmento de Fśica y Astronomá, Universidad de Valparaśo, Avenida Gran Bretana 1111, Valparaíso 2360102, Chile*

Accepted 2014 September 8. Received 2014 September 4; in original form 2014 July 18

ABSTRACT

We present the discovery of strongly variable emission lines from a gaseous disc around the DA white dwarf SDSS J1617+1620, a star previously found to have an infrared excess indicative of a dusty debris disc formed by the tidal disruption of a rocky planetary body. Time series spectroscopy obtained during the period 2006–2014 has shown the appearance of strong double-peaked Ca II emission lines in 2008. The lines were weak, at best, during earlier observations, and monotonically faded through the remainder of our monitoring. Our observations represent unambiguous evidence for short-term variability in the debris environment of evolved planetary systems. Possible explanations for this extraordinary variability include the impact on to the dusty disc of either a single small rocky planetesimal, or of material from a highly eccentric debris tail. The increase in flux from the emission lines is sufficient that similar events could be detected in the broad-band photometry of ongoing and future large-area time domain surveys.

Key words: circumstellar matter – stars: individual: SDSS J1617+1620 – planetary systems – white dwarfs.

1 INTRODUCTION

In 1987, an infrared (IR) excess was discovered around the metal-polluted white dwarf GD29-38 (Zuckerman & Becklin 1987). Initially thought to have been evidence of a brown dwarf companion, it was later shown by Graham et al. (1990) to be emission from a dusty disc in orbit around the white dwarf, formed by the tidal disruption of an asteroid (Jura 2003). Since then similar IR excesses have been detected around ≃30 more white dwarfs, and current estimates suggest that 1–3 per cent of white dwarfs possess dusty debris discs (Farihi, Jura & Zuckerman 2009; Girven et al. 2011; Steele et al. 2011). Accretion from the debris discs results in metal pollution of the white dwarf atmospheres (Koester, Provencal & Shipman 1997), opening up a window on the bulk abundances of exoplanetary material (Zuckerman et al. 2007; Klein et al. 2010; Dufour et al. 2012; Gänsicke et al. 2012; Jura et al. 2012; Xu et al. 2013; Barstow et al. 2014). Interestingly, the fraction of white dwarfs exhibiting traces of metals in their atmospheres is 25–50 per cent (Zuckerman et al. 2003, 2010; Koester, Gänsicke & Farihi 2014), suggesting that circumstellar debris too tenuous for detection with current instrumentation is very frequent (see also Bergfors et al. 2014).

In addition to circumstellar dust, gaseous metallic discs have been found around a handful of metal-polluted white dwarfs through the detection of emission lines of the 8600Å Ca II triplet (Gänsicke et al. 2006, 2008; Gänsicke, Marsh & Southworth 2007; Gänsicke 2011; Dufour et al. 2012; Farihi et al. 2012; Melis et al. 2012). The double-peaked morphology of the Ca II lines dynamically constrains the gas to be located within the Roche radius of the white dwarf, with the inner disc radii being a few ten white dwarf radii, broadly consistent with the sublimation radius (but see Rafikov & Garmilla 2012). Brinkworth et al. (2009, 2012) and Melis et al. (2010) showed that the gaseous and dusty disc components overlap largely in their radial extension, which is intriguing as the temperature beyond the sublimation radius should not be sufficiently high to produce the gaseous disc (Hartmann et al. 2011). In addition to this, we do not observe gaseous discs at all white dwarfs with IR excess (Farihi et al. 2012), which suggests that the production mechanism of the gaseous discs is not universal. Plausible scenarios for the generation of gas are collisions of multiple asteroids (Jura 2008) and sublimation that may lead to a runaway evolution of the debris discs (Rafikov 2011; Metzger, Rafikov & Bochkarev 2012).

All the above suggests that the detection of gaseous discs around metal-polluted white dwarfs may point to a highly dynamic debris

★ E-mail: d.j.wilson.1@warwick.ac.uk

Table 1. Log of observations SDSS J1617+1620.

Date	Telescope/ instrument	Wavelength range (Å)	Spectral resolution (Å)	Total exposure time (s)
2006 July 01	SDSS	3800–9200	0.9	5700
2008 March 03	SDSS	3800–9200	0.9	14 700
2009 February 17	WHT	3690–8890	1.6	3600
2010 April 23	WHT	3630–8850	0.5	3600
2010 June 10	Gemini N	7750–8960	0.7	3600
2011 March 21	X-shooter	2990–24790	0.2	6990
2011 May 31	X-shooter	2990–24790	0.2	16 380
2011 June 05	X-shooter	2990–24790	0.2	8190
2013 May 05	UVES	3760–9440	0.05	4800
2014 April 30	FORS	7750–9550	0.8	900

environment. So far, evidence for short-term observational variability of debris discs is very limited. Gänsicke et al. (2008) reported changes in the line profile shapes of the Ca II emission lines detected in SDSS J084539.17+225728.0, and von Hippel & Thompson (2007) claimed variability in the strength of the Ca K 3934 Å absorption line in the prototype GD 29−38, though the latter result was disputed (Debes & López-Morales 2008). The strongest evidence for variability previously observed in such systems is the drop in the IR luminosity of the dusty debris disc around WD J0959-0200 in 2010 (Xu & Jura 2014).

Here, we report the discovery of a strongly variable gaseous disc around the metal-polluted white dwarf SDSS J161717.04+162022.4.

2 DISCOVERY

We applied the procedure outlined in Gänsicke et al. (2008) to search for white dwarfs with Ca II emission in Data Release (DR) 7 of the Sloan Digital Sky Survey (SDSS; Abazajian et al. 2009), and identified two new systems, the He-atmosphere (DB) SDSS J073842.56+183509.6 (see also Dufour et al. 2012) and the H-atmosphere (DA) SDSS J161717.04+162022.4 (henceforth SDSS J1617+1620; Gänsicke 2011). The SDSS spectrum revealed Mg II 4481 Å absorption in the white dwarf atmosphere, and *Spitzer* observations of SDSS J1617+1620 confirmed the expected presence of circumstellar dust (Brinkworth et al. 2012).

The DR 7 spectrum of SDSS J1617+1620 was obtained on 2008 March 3. Only later, we realized that the star had an earlier DR 6 (Adelman-McCarthy et al. 2008) spectrum, obtained on 2006 July 1 – in which the Ca II emission lines are weakly detected, at best. Intrigued by this clear evidence for variability, we initiated spectroscopic monitoring, using the William Herschel Telescope (WHT), Gemini North, and the ESO Very Large Telescope (VLT).

3 FOLLOW-UP OBSERVATIONS

The log of the observations is given in Table 1. The first follow-up spectra of SDSS J1617+1620 were obtained using the Intermediate dispersion Spectrograph and Imaging System spectrograph mounted on the WHT, with observations carried out on 2009 February 17 and 2010 April 23. On both occasions two 1800 s exposures were taken, with a third 540 s exposure obtained in 2010. Observations were obtained simultaneously through the blue and red arms of the instrument. The CCDs were binned by factors of 2 (spectral) and 3 (spatial) to limit the impact of readout noise on the observations. The blue arm was equipped with the R600B grating and had a wavelength coverage of 3690–4110 Å at a reciprocal dispersion of 0.45 Å per binned pixel and a resolution of approximately 1 Å. The red arm had the R316R grating in 2009, covering 5760–8890 Å with a reciprocal dispersion of 1.85 Å per binned pixel and a resolution of approximately 3.5 Å, and the R1200R grating in 2010, with a reciprocal dispersion of 1.52 Å per binned pixel and a resolution of approximately 1.1 Å. The data were reduced and the spectra optimally extracted using the PAMELA[1] code (Marsh 1989) and the STARLINK[2] packages FIGARO and KAPPA. Copper–neon and copper–argon arc lamp exposures were taken before and after the observations and the wavelength calibrations were linearly interpolated from them. We removed the telluric lines and flux-calibrated the target spectra using observations of BD +75 325 in 2007 and SP1036+433 in 2010.

The next observations were obtained on 2010 June 10 at the Gemini North Telescope, where four 900 s exposures were obtained in the *i* band using the R831 grating, with a central wavelength setting of 8600 Å. The CCDs were binned by a factor of 2 × 2 and the wavelength was calibrated using CuAr arcs taken at the end of the night. As with the WHT images, the spectra were again reduced using standard STARLINK procedures, and then optimally extracted using PAMELA. The wavelength calibration was done using MOLLY.

Observations at the VLT with X-shooter (Vernet et al. 2011) in 2011 March–June and the Ultraviolet and Visual Echelle Spectrograph (UVES; Dekker et al. 2000) on 2013 May 05 were reduced using the REFLEX[3] software developed by ESO. The X-shooter data were reduced using the REFLEX Nod mode, with the various parameters of the reduction pipeline varied using trial and error to produce the best possible spectra. For the UVES data, the default REFLEX settings were found to be sufficient. After this a heliocentric correction was applied to the REFLEX products. Where multiple observations were made on the same night the spectra were combined using a weighted average.

A final VLT observations was obtained with the FOcal Reducer and low dispersion Spectrograph (FORS; Appenzeller et al. 1998), taking three long-slit spectra of 300 s exposures on 2014 April 30. We covered the near-IR spectral range (7750–9250 Å), using the standard resolution collimator (2 × 2), the dispersion grism GRIS_1028z+29, and the order separator filter OG590 that give

[1] PAMELA and MOLLY were written by T. R. Marsh and can be obtained from http://www.warwick.ac.uk/go/trmarsh

[2] The STARLINK software and documentation can be obtained from http://starlink.jach.hawaii.edu/

[3] The REFLEX software and documentation can be obtained from http://www.eso.org/sci/software/reflex/

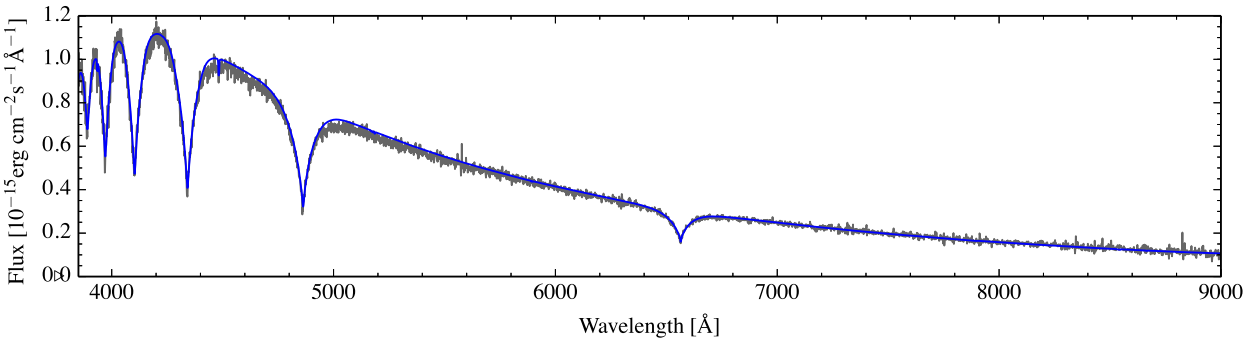

Figure 1. Spectrum of SDSS J1617+1620 obtained by SDSS in 2006 (grey). The atmospheric parameters, $T_{\rm eff} = 13520 \pm 200$ K and $\log g = 8.11 \pm 0.08$, were determined by averaging the fits to both SDSS spectra. The corresponding model spectrum is shown in blue. Photospheric absorption of Ca K 3934 Å and Mg II 4481 Å is detected in both SDSS spectra.

a dispersion of 0.8 Å pixel^{-1}, which corresponds to a resolving power $R \sim 3800$ at 8500 Å. We reduced the data in a standard fashion, using traditional IRAF routines for long-slit spectroscopy, i.e. the three spectra were bias-subtracted, flat-fielded, wavelength-calibrated, sky-subtracted, flux-calibrated, and finally combined. The spectrophotometric standard G138-31 was observed soon after SDSS J1617+1620 at similar airmass, although the night was not photometric and only relative flux calibration has been possible.

Comparing the two SDSS spectra (Fig. 2) shows the dramatic increase in the strength of the Ca II 8600 Å emission line triplet between 2006 and 2008, revealing the formation of a gaseous disc around SDSS J1617+1620. The WHT observations, less than a year later, show a significant reduction in the strength of the emission lines, as does the Gemini spectra.

The X-shooter spectra show a further decrease in the strength of the Ca II triplet from the WHT and Gemini data, although the emission lines were still clearly visible on this occasion. However, by the time of the UVES observation in 2013 the emission lines appear to have disappeared below the detection threshold. Thanks to the high resolution of the VLT instruments the Ca K 3934 Å and Mg II 4481 Å absorption lines are clearly detected and well defined, allowing for an accurate measurement of the metal abundances in the atmosphere of SDSS J1617+1620.

The FORS spectrum, as with the UVES observations a year before, shows no indication of the Ca II 8600 Å emission lines, confirming the disappearance of the gaseous disc.

4 WHITE DWARF PARAMETERS

The atmospheric parameters of SDSS1617+1620 were calculated by fitting model spectra to the SDSS spectroscopy (Fig. 1) as described by Koester (2010). We report the average parameters obtained from the two SDSS spectra, estimating the uncertainty from the discrepancy between the two fits, as $T_{\rm eff} = 13\,520 \pm 200$ K and $\log g = 8.11 \pm 0.08$. The corresponding mass, radius, and cooling age, computed from the hydrogen-atmosphere cooling models of Bergeron and collaborators,[4] are $M_{\rm wd} = 0.68 \pm 0.05\,{\rm M}_{\odot}$, $R_{\rm wd} = 0.0120 \pm 0.007\,{\rm R}_{\odot}$, and $T_{\rm cool} = 350 \pm 50$ Myr. Using the initial-mass to final-mass relations of Catalán et al. (2008), Kalirai et al. (2008), Williams, Bolte & Koester (2009), and Casewell et al. (2009) suggests a main-sequence progenitor mass of 2.2–3.0 $\rm M_{\odot}$, similar to the majority of the metal-polluted white dwarfs (Jura & Xu 2012; Koester et al. 2014).

[4] http://www.astro.umontreal.ca/~bergeron/CoolingModels, based on Holberg & Bergeron (2006), Kowalski & Saumon (2006), Tremblay, Bergeron & Gianninas (2011).

5 VARIABILITY OF THE CA II TRIPLET

The dramatic change in the strength of the Ca II emission lines is illustrated in Fig. 2, where the triplet is clearly seen in the second SDSS spectrum (MJD = 54557), and subsequently fades during our follow-up spectroscopy. To quantify the variable nature of the gaseous disc, we measure the equivalent widths of the emission lines. As the 8542 and 8662 Å components overlap in some of the spectra, we computed the combined equivalent width of the entire triplet, using the wavelength range 8460–8700 Å. The resulting values are sensitive to the method used to fit the underlying continuum, leading to systematic uncertainties that dominate the error budget in the case of weak or non-existing line emission. The equivalent widths reported in Table 2, and shown in Fig. 3, confirm the appearance of strong Ca II emission lines in 2008, which subsequently faded by a factor $\simeq$2.5 within less than a year. The decline in the strengths of the lines then slowed down, and our last spectrum obtained in 2014 April is consistent with the complete disappearance of the lines. Unfortunately, the onset of the Ca II emission is not well-documented. While our analysis formally detects the Ca II triplet in the 2006, the corresponding SDSS spectrum is overall of relatively poor quality, and more specifically the wavelength range relevant for the equivalent measurement is affected by residuals from the sky line subtraction. We are therefore unable to unambiguously say whether a gaseous disc was present already in 2006, or if it only formed in 2008.

Assuming that the dispersion of the gaseous disc by 2014 was due to viscous angular momentum exchange suggests a viscous timescale $t_{\rm v} \approx 8$ yr. Using equation 2 of Metzger et al. (2012) yields a viscosity parameter $\alpha \sim 0.25$, within the range estimated by King, Pringle & Livio (2007) for an ionized thin disc.

The Ca II lines show a mildly-double-peaked morphology (Fig. 2), which arises from the Doppler shifts induced by the Keplerian velocity of the material in the disc (Horne & Marsh 1986). The total width and peak separation of the Ca II lines can be used to estimate the inner and outer radii of the disc, respectively, and we find $R_{\rm in} \sin^2 i \approx 0.5\,{\rm R}_{\odot}$ and $R_{\rm out} \sin^2 i \approx 1.2\,{\rm R}_{\odot}$, where i is the unknown inclination of the disc. These values are similar to the inner and outer radius estimated for SDSS J122859.93+104032.9 and SDSS J084539.17+225728.0 (Gänsicke et al. 2006, 2008), i.e. the outer radius is compatible with the tidal disruption radius of a

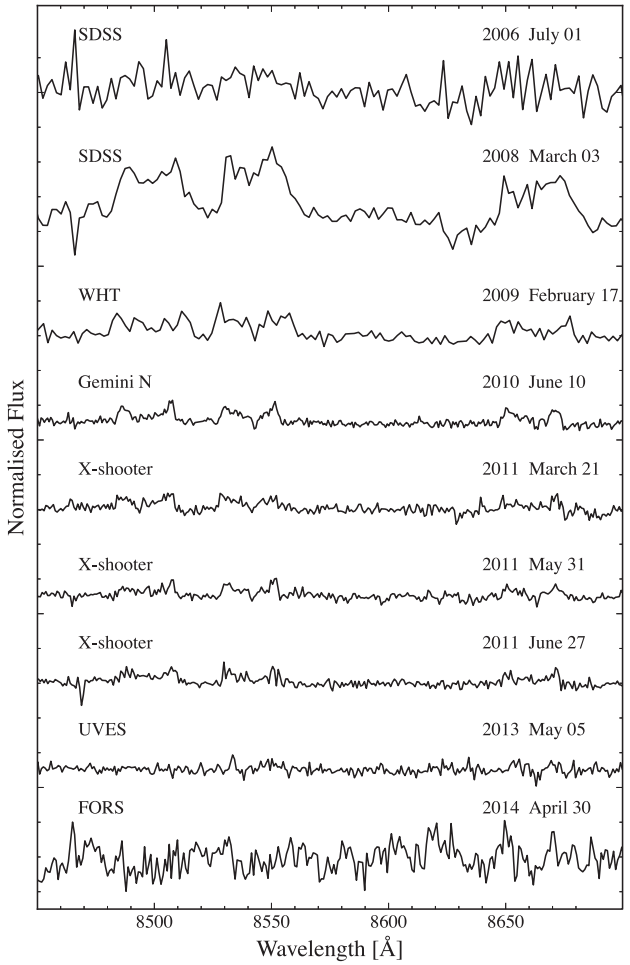

Figure 2. Normalized time series spectroscopy of SDSS J1617+1620 showing the change in strength of the Ca II 8600 Å emission line triplet between 2006 and 2014. The telescope/instrument used to make the observation is indicated on the left above each spectrum, with the date of the observation on the right. On earlier dates the lines clearly show the double-peaked morphology characteristic of emission from a gaseous disc around the white dwarf (Horne & Marsh 1986). However by the time that the UVES spectrum was obtained in 2013 March the lines, and hence the gaseous disc, had disappeared (Fig. 3).

rocky asteroid (Davidsson 1999), and the inner radius is near the sublimation radius (von Hippel et al. 2007). Note that, whilst the inner radius can be constrained by calculating the Doppler shift at the full width zero intensity of the emission lines, the point with represents the outer edge is somewhat more arbitrary. In this case, we chose to measure the peak separation of the lines to provide a lower limit.

Inspecting our WHT, Gemini, and VLT/X-shooter spectra, there is a slight hint that the width of the Ca II lines decreases with time, which would imply the inner radius of the gas disc moving further out. However, the emission lines in the later observations are too weak to make a firm conclusion.

6 ACCRETION OF PLANETARY MATERIAL

In addition to the Ca II 8600 Å emission line triplet, we detect photospheric absorption of Ca K 3934 Å and Mg II 4481 Å (Fig. 4). The detection of metal pollution provides an opportunity to investigate the chemical diversity of extrasolar planetary systems (e.g. Zuckerman et al. 2007; Klein et al. 2011; Gänsicke et al. 2012; Xu et al. 2014). The relevant procedures and detailed physics have been extensively described by Gänsicke et al. (2012) and Koester et al. (2014), and we provide here only a brief summary.

A key assumption in the interpretation of the photospheric metal abundances is a steady state between accretion and diffusion (Koester 2009), in which case the diffusion flux is constant throughout the atmosphere, and equal to the accretion rate from the debris disc. The relativity low effective temperature of SDSS J1617+1620 implies that the diffusion of metals within the atmosphere of should not be affected by radiative levitation (Chayer, Fontaine & Wesemael 1995). While the temperature is sufficiently high that no deep convection zone develops, some convection zones are present

Table 2. Equivalent widths of the absorption and emission lines in the times-series spectra of SDSS J1617+1620. Note the relative consistency of the Ca K 3934 Å and Mg II 4481 Å absorption lines compared to the hugely variable Ca II 8600 Å triplet. No measurement was made of the absorption lines in four cases: the SDSS spectra are of insufficient quality for an accurate measurement, and the Gemini and FORS observations did not cover the corresponding wavelength range.

	Equivalent width [Å]		
Date	Ca II 3934 Å	Mg II 4481 Å	Ca II 8600 Å Triplet
2006 July 01	–	–	-6.4 ± 1.8
2008 March 03	–	–	-16.1 ± 1.2
2009 February 17	0.20 ± 0.02	0.34 ± 0.02	-6.1 ± 1.0
2010 April 23	0.16 ± 0.03	0.36 ± 0.05	-4.2 ± 1.0
2010 June 10	–	–	-3.4 ± 0.8
2011 March 21	0.21 ± 0.01	0.30 ± 0.02	-3.3 ± 0.8
2011 May 31	0.20 ± 0.01	0.28 ± 0.01	-2.6 ± 0.8
2011 June 27	0.20 ± 0.01	0.26 ± 0.01	-2.8 ± 0.8
2013 May 05	0.23 ± 0.01	0.26 ± 0.01	-1.5 ± 1.1
2014 April 30	–	–	-0.9 ± 0.9

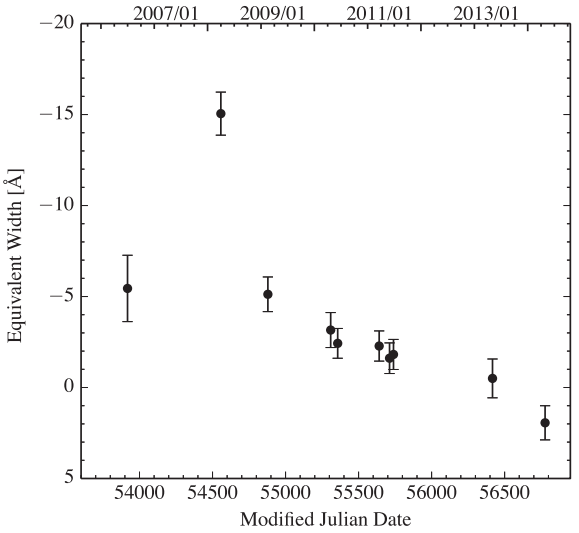

Figure 3. Change in the strength of the Ca II triplet seen in the spectra of SDSS J1617+1620 over the period 2006–2014 (Fig. 2). The equivalent widths of the emission lines in each spectrum were calculated over the wavelength range 8460–8700 Å. The strength of the emission line increases by a factor ∼3 between the first and second observations, before dropping down to zero by 2013. This represents a dramatic increase then loss of emission from a gaseous disc around SDSS J1617+1620.

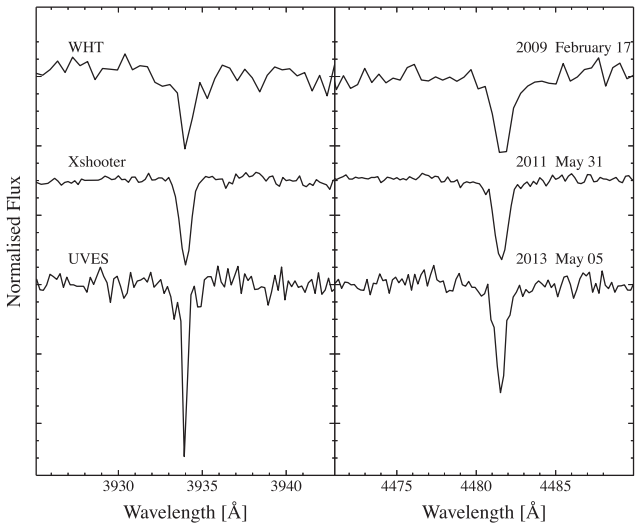

Figure 4. Photospheric absorption lines of Ca K 3934 Å (left) and Mg II 4481 Å (right), illustrating the different spectral resolutions of the instruments used for the follow-up spectroscopy. The equivalent widths measured from all our spectra are given in Table 2 and average accretion fluxes are given in Table 3. The apparent greater depth of the UVES observation of the Ca K line is an effect of the spectral resolution and does not represent an increase in equivalent width.

Table 3. Diffusion time-scales and average accretion fluxes, computed under the assumption of a fully convective atmosphere or using the diffusion time-scales at the bottom of the shallow convection zone near the surface.

Element	Fully convective		Convective at $\tau_R = 3.2$	
	$\log \tau_{diff}$ (yr)	$\dot{m}$(g s^{-1})	$\log \tau_{diff}$ (yr)	$\dot{m}$(g s^{-1})
12 Mg	−0.46	1.7×10^8	−2.2	7.3×10^7
14 Si	−0.36	$\leq 2.5 \times 10^8$	−2.5	$\leq 2.9 \times 10^8$
20 Ca	−0.37	7.2×10^6	−2.3	5.0×10^6

at Rosseland optical depths $0.04 \lesssim \tau_R \lesssim 3.2$ and $300 \lesssim \tau_R \lesssim 1936$. In between these zones the atmosphere is radiative. Regardless of the details of the atmospheric structure, the diffusion time-scales are very short ($\tau_{diff} \approx 0.5$ yr, Table 3), meaning that SDSS J1617+1620 must be currently accreting from an external source, almost certainly the circumstellar gas and dust. We have computed the corresponding diffusion fluxes under two assumptions: (1) treating the entire atmosphere as convective and (2) evaluating the diffusion time-scales at $\tau_R = 3.2$, the bottom of the shallow convection zone near the surface.

Table 3 reports the average accretion fluxes of Mg and Ca, and an upper limit for Si, obtained from the analysis our WHT, X-Shooter, and UVES spectra (the quality of the SDSS spectra is too low, and the Gemini and FORS spectra do not cover the relevant wavelength range). Scaling for the relative abundance of Mg and Ca in the bulk Earth (Allègre, Manhès & Lewin 2001), we estimate a total metal accretion flux on to the white dwarf of $\approx (6.4 \pm 1.8$–$7.8 \pm 3.3) \times 10^8$ g s^{-1}, consistent with the accretion rates measured in other dusty DA white dwarfs (Vennes, Kawka & Németh 2010, 2011; Melis et al. 2011; Gänsicke et al. 2012).

We find that the planetary debris around SDSS J1617+1620 has $\log$[Ca/Mg] $= -1.4$ to -1.6, (by number, depending on the treatment of convection), which is somewhat low compared to the values found for the bulk Earth (−1.17; McDonough 2000) C I chondrites (−1.24; Lodders 2003), and the Sun (−1.24; Lodders 2003). A depletion relative to other elements is also seen in GALEX J193156.8+011745 (Vennes et al. 2010, 2011; Melis et al. 2011; Gänsicke et al. 2012), and was interpreted by Melis et al. (2011) as potential evidence for the accretion of a differentiated body that had its crust and part of its mantle stripped. Conclusions regarding the nature and origin of the debris around SDSS J1617+1620 remain very limited as only two photospheric elements are so far detected. Progress will require deep optical and ultraviolet spectra probing for the abundances of C, Si, Al, Ti, and Fe.

A final note concerns the temporal evolution of the photospheric absorption lines of Mg and Ca. While the equivalent widths of the Ca K line are constant within the uncertainties (Table 2), the Mg II 4481 Å lines shows a notionally significant change, being strongest in the first WHT observation during the early decline of the Ca II emission lines. Rafikov (2011) and Metzger et al. (2012) showed that the generation of gas can lead to a significant increase in the accretion on to the white dwarf. While the observations do not exclude small changes in the accretion rate of Mg (which, if real, would imply a chemical differentiation within the debris), they do rule out a large variation of the total accretion rate.

7 DISCUSSION

The formation mechanism of gaseous discs around metal-polluted white dwarfs is very uncertain. Gaseous discs are only observed around a small fraction of the metal-polluted white dwarfs, and in all cases where Ca II emission lines are observed circumstellar dust is also detected in the form of a noticeable IR excess (Brinkworth et al. 2009, 2012; Melis et al. 2010, 2012; Farihi et al. 2012). However, many dusty and strongly metal-polluted white dwarfs do not show any emission lines from circumstellar gas (e.g. Gänsicke et al. 2007; Vennes et al. 2010; Klein et al. 2011; Farihi et al. 2012), so their formation cannot be universal. Gaseous discs are found around white dwarfs with temperatures ranging from $\simeq 13\,000$ to $\simeq 22\,000$ K (Gänsicke et al. 2006, 2007, 2008; Dufour et al. 2012; Farihi et al. 2012; Melis et al. 2012), very similar to the range where dusty discs are found (Farihi et al. 2009).

The Ca II emission lines can be modelled by optically thin H and He-deficient gas with a temperature near 6000 K, but the heating mechanism is unclear: Hartmann et al. (2011) assume an active disc, i.e. heated by the inwards flow of material, but require an unrealistically high accretion rate of 10^{17-18} g s^{-1}, which is many orders of magnitude higher than the accretion rates on to the white dwarf derived from the photospheric abundances. Kinnear (2011) and Melis et al. (2010) showed that irradiation from the white dwarf is sufficient to keep circumstellar metal gas at many 1000 K, and that cooling occurs primarily through optically thick lines. Kinnear (2011) could quantitatively reproduce the observed line fluxes with a photoionization model.

The high temperature necessary to explain the Ca II emission lines, together with the radial extent of the gas discs ($\sim$0.5–1.5 $R_\odot$) and the absence of gas at many dusty white dwarfs rules out production of the gas by sublimation of the dust within the radiation field of the white dwarf. In fact Gänsicke et al. (2006, 2007) and Brinkworth et al. (2012) showed that the location of the inner edges of the gas discs derived from observations are broadly consistent with the sublimation radius, i.e. the radial distribution of gas and dust largely overlap (for completeness, we note that line-of-sight absorption of circumstellar gas has been detected in two cases, see

Debes et al. 2012b; Gänsicke et al. 2012, but the exact location of that gas is not well known).

We speculate on two possible explanations for the transient formation of the gaseous disc. One scenario is the impact of a small asteroid on to a more massive, pre-existing debris disc (Jura 2008). The rocky nature of this body is implied by the absence of Balmer emission lines from the disc. Entering the tidal disruption radius, the incoming asteroid will start to break up, and vaporize upon the high-velocity impact on to the disc. The gas generated in that way will subsequently spread radially due to viscous angular momentum exchange, and heating by the white dwarf will result in the observed Ca II emission. The gas will eventually accrete on to the white dwarf (with a small amount moving outwards to carry away angular momentum), and the decreasing density will result in a weakening of the emission lines. In summary, such a 'secondary impact' event would be produce a single event of transient Ca II emission.

A slight twist to the above scenario is that the dust disc at SDSS J1617+1620 is young, and we have witnessed the impact of material in a debris tail leftover from the original disruption. The detailed evolution of the tidal disruption of asteroids has not yet been fully explored. Debes, Walsh & Stark (2012a) simulated the disruption of a rubble pile asteroid, and found that an elongated debris train is formed. Veras et al. (2014) followed the evolution of a disrupted rubble piles over many orbital cycles, and demonstrated that, in the absence of additional forces beyond gravity, a highly collisionless eccentric ring of debris is formed. Additional forces, e.g. from sublimation, are probably required to fan out the debris train, eventually circularising material in a close-in circumstellar disc. This process is likely to extend over many orbital cycles, which, as the original semimajor axis of the asteroid should have been >1–2 au (i.e. beyond the region cleared out during the red giant phase), could imply time-scales of many tens to even thousands of years. During that period, repeated impacts of leftover debris are expected, and one would expect another flare-up of gas emission from SDSS J1617+1620 over the next years to decade.

The serendipitous discovery of the transient Ca II emission in SDSS J1617+1620 is a strong motivation for a more systematic monitoring of large numbers of white dwarfs to detect tidal disruption events of planetary bodies. The spectroscopic observations that led to the discovery of the gas disc in SDSS J1617+1620 are moderately expensive in terms of telescope time and aperture. The observed changes in the Ca II line fluxes correspond to a 2 per cent variability of SDSS J1617+1620 in the z band. Such events are hence close to the detection threshold of current ground-based transient surveys (Ivezić et al. 2007; Ofek et al. 2012), but should be easily detected in the era of *Gaia* and LSST (LSST Science Collaboration et al. 2009; Carrasco et al. 2014).

8 CONCLUSION

We have observed unambiguous evidence for a variable gaseous disc around the white dwarf SDSS J1617+1620, demonstrating that observations of dusty and gaseous discs around metal-polluted white dwarfs can provide further insight into the dynamics of such systems. This will also allow us to explore the nature and composition of the accreted material in greater detail and better understand the post-main-sequence evolution of extrasolar planetary systems. Continued observations of SDSS J1617+1620 and other white dwarfs with gaseous discs will be required to further investigate the highly dynamical nature of evolved planetary systems.

ACKNOWLEDGEMENTS

The research leading to these results has received funding from the European Research Council under the European Union's Seventh Framework Programme (FP/2007-2013)/ERC Grant Agreement no. 320964 (WDTracer). BTG was supported in part by the UK's Science and Technology Facilities Council (ST/I001719/1). DJW would like to thank M Hollands for help with Figure (1).

This paper has made use of observations from the SDSS-III, funding for which has been provided by the Alfred P. Sloan Foundation, the Participating Institutions, the National Science Foundation, and the US Department of Energy Office of Science. It is also based on observations made with the WHT on the island of La Palma by the Isaac Newton Group in the Spanish Observatorio del Roque de los Muchachos of the Instituto de Astrofísica de Canarias, spectra obtained with the Gemini North Telescope under programme GN-2010A-Q-94, and observations made with ESO Telescopes at the La Silla Paranal Observatory under programme ID 093.D-0838(A), 087.D-0139(C), 091.D-0296(A), and 386.C-0218(E).

REFERENCES

Abazajian K. N. et al., 2009, ApJS, 182, 543
Adelman-McCarthy J. K. et al., 2008, ApJS, 175, 297
Allègre C., Manhès G., Lewin E., 2001, Earth Planet. Sci. Lett., 185, 49
Appenzeller I. et al., 1998, The Messenger, 94, 1
Barstow M. A., Barstow J. K., Casewell S. L., Holberg J. B., Hubeny I., 2014, MNRAS, 440, 1607
Bergfors C., Farihi J., Dufour P., Rocchetto M., 2014, 444, 2147
Brinkworth C. S., Gänsicke B. T., Marsh T. R., Hoard D. W., Tappert C., 2009, ApJ, 696, 1402
Brinkworth C. S., Gänsicke B. T., Girven J. M., Hoard D. W., Marsh T. R., Parsons S. G., Koester D., 2012, ApJ, 750, 86
Carrasco J. M., Catalán S., Jordi C., Tremblay P.-E., Napiwotzki R., Luri X., Robin A. C., Kowalski P. M., 2014, A&A, 565, A11
Casewell S. L., Dobbie P. D., Napiwotzki R., Burleigh M. R., Barstow M. A., Jameson R. F., 2009, MNRAS, 395, 1795
Catalán S., Isern J., García-Berro E., Ribas I., 2008, MNRAS, 387, 1693
Chayer P., Fontaine G., Wesemael F., 1995, ApJS, 99, 189
Davidsson B. J. R., 1999, Icarus, 142, 525
Debes J. H., López-Morales M., 2008, ApJ, 677, L43
Debes J. H., Walsh K. J., Stark C., 2012a, ApJ, 747, 148
Debes J. H., Kilic M., Faedi F., Shkolnik E. L., Lopez-Morales M., Weinberger A. J., Slesnick C., West R. G., 2012b, ApJ, 754, 59
Dekker H., D'Odorico S., Kaufer A., Delabre B., Kotzlowski H., 2000, in Iye M., Moorwood A. F., eds, Proc. SPIE Conf. Ser. Vol. 4008, Optical and IR Telescope Instrumentation and Detectors. SPIE, Bellingham, p. 534
Dufour P., Kilic M., Fontaine G., Bergeron P., Melis C., Bochanski J., 2012, ApJ, 749, 6
Farihi J., Jura M., Zuckerman B., 2009, ApJ, 694, 805
Farihi J., Gänsicke B. T., Steele P. R., Girven J., Burleigh M. R., Breedt E., Koester D., 2012, MNRAS, 421, 1635
Gänsicke B. T., 2011, in Schuh S., Drechsel H., Heber U., eds, AIP Conf. Proc. Vol. 1331, Planetary Systems Beyond the MAIN Sequence. Am. Inst. Phys., New York, p. 211
Gänsicke B. T., Marsh T. R., Southworth J., Rebassa-Mansergas A., 2006, Science, 314, 1908
Gänsicke B. T., Marsh T. R., Southworth J., 2007, MNRAS, 380, L35
Gänsicke B. T., Koester D., Marsh T. R., Rebassa-Mansergas A., Southworth J., 2008, MNRAS, 391, L103
Gänsicke B. T., Koester D., Farihi J., Girven J., Parsons S. G., Breedt E., 2012, MNRAS, 424, 333
Girven J., Gänsicke B. T., Steeghs D., Koester D., 2011, MNRAS, 417, 1210
Graham J. R., Matthews K., Neugebauer G., Soifer B. T., 1990, ApJ, 357, 216

Hartmann S., Nagel T., Rauch T., Werner K., 2011, A&A, 530, A7
Holberg J. B., Bergeron P., 2006, AJ, 132, 1221
Horne K., Marsh T. R., 1986, MNRAS, 218, 761
Ivezić Ž. et al., 2007, AJ, 134, 973
Jura M., 2003, ApJ, 584, L91
Jura M., 2008, AJ, 135, 1785
Jura M., Xu S., 2012, AJ, 143, 6
Jura M., Xu S., Klein B., Koester D., Zuckerman B., 2012, ApJ, 750, 69
Kalirai J. S., Hansen B. M. S., Kelson D. D., Reitzel D. B., Rich R. M., Richer H. B., 2008, ApJ, 676, 594
King A. R., Pringle J. E., Livio M., 2007, 376, 1740
Kinnear T., 2011, Master's thesis, Univ. Warwick
Klein B., Jura M., Koester D., Zuckerman B., Melis C., 2010, ApJ, 709, 950
Klein B., Jura M., Koester D., Zuckerman B., 2011, ApJ, 741, 64
Koester D., 2009, A&A, 498, 517
Koester D., 2010, Mem. Soc. Astron. Ital., 81, 921
Koester D., Provencal J., Shipman H. L., 1997, A&A, 320, L57
Koester D., Gänsicke B. T., Farihi J., 2014, A&A, 566, A34
Kowalski P. M., Saumon D., 2006, ApJ, 651, L137
Lodders K., 2003, ApJ, 591, 1220
et al. LSST Science Collaboration, 2009, preprint (arXiv:0912.0201)
McDonough W., 2000, in Teisseyre R., Majewski E., eds, Earthquake Thermodynamics and Phase Transformation in the Earth's Interior. Elsevier, Amsterdam, p. 5
Marsh T. R., 1989, PASP, 101, 1032
Melis C., Jura M., Albert L., Klein B., Zuckerman B., 2010, ApJ, 722, 1078
Melis C., Farihi J., Dufour P., Zuckerman B., Burgasser A. J., Bergeron P., Bochanski J., Simcoe R., 2011, ApJ, 732, 90
Melis C. et al., 2012, ApJ, 751, L4
Metzger B. D., Rafikov R. R., Bochkarev K. V., 2012, MNRAS, 423, 505
Ofek E. O. et al., 2012, PASP, 124, 62
Rafikov R. R., 2011, MNRAS, 416, L55
Rafikov R. R., Garmilla J. A., 2012, ApJ, 760, 123
Steele P. R., Burleigh M. R., Dobbie P. D., Jameson R. F., Barstow M. A., Satterthwaite R. P., 2011, MNRAS, 416, 2768
Tremblay P.-E., Bergeron P., Gianninas A., 2011, ApJ, 730, 128
Vennes S., Kawka A., Németh P., 2010, MNRAS, 404, L40
Vennes S., Kawka A., Németh P., 2011, MNRAS, 413, 2545
Veras D., Leinhardt Z., Bonsor A., Gänsicke B., 2014, MNRAS, in press
Vernet J. et al., 2011, A&A, 536, A105
von Hippel T., Thompson S. E., 2007, ApJ, 661, 477
von Hippel T., Kuchner M. J., Kilic M., Mullally F., Reach W. T., 2007, ApJ, 662, 544
Williams K. A., Bolte M., Koester D., 2009, ApJ, 693, 355
Xu S., Jura M., 2014, preprint (arXiv:e-prints)
Xu S., Jura M., Klein B., Koester D., Zuckerman B., 2013, ApJ, 766, 132
Xu S., Jura M., Koester D., Klein B., Zuckerman B., 2014, ApJ, 783, 79
Zuckerman B., Becklin E. E., 1987, Nature, 330, 138
Zuckerman B., Koester D., Reid I. N., Hünsch M., 2003, ApJ, 596, 477
Zuckerman B., Koester D., Melis C., Hansen B. M., Jura M., 2007, ApJ, 671, 872
Zuckerman B., Melis C., Klein B., Koester D., Jura M., 2010, ApJ, 722, 725

This paper has been typeset from a TEX/LATEX file prepared by the author.